Available online at www.sciencedirect.com
SCIENCE DIRECT®
Physica B 369 (2005) 293–298
PHYSICA B
www.elsevier.com/locate/physb

Multichannel model of magnetotunneling in disordered electron nanodevices

M. Amado[a], F. Domínguez-Adame[a,*], E. Diez[b]

[a]GISC, Departamento de Física de Materiales, Universidad Complutense, E-28040 Madrid, Spain
[b]Área de Física Teórica, Universidad de Salamanca, E-37008 Salamanca, Spain

Received 19 May 2005; received in revised form 26 August 2005; accepted 26 August 2005

Abstract

We present a multichannel model of magnetotunneling transport in unintentionally disordered double-barrier GaAs-$Al_xGa_{1-x}As$ heterostructures. The source of disorder comes from interface roughness at the heterojunctions. Disorder break translational symmetry along the lateral direction and therefore electrons can be scattered off the growth direction. The model correctly describes channel mixing due to these elastic scattering events. The magnetic field applied to the double-barrier heterostructure splits the resonant level into a set of equally-spaced resonances, the level spacing increasing with the magnetic field. We discuss the influence of the various parameters (epilayer widths and magnitude or disorder) on the lineshape of the resonant levels.

PACS: 78.30.Ly; 73.40.Gk; 73.30.+y

Keywords: Disordered solids; Tunneling; Magnetotransport

1. Introduction

Recent advances in nanofabrication techniques, such as molecular beam epitaxy, make it possible to fabricate solid-state devices with high crystalline quality. By these means, a large variety of heterostructures were designed for both basic and applied physics. Among them, resonant tunneling devices based on double-barrier structures (DBs) are currently under extensive investigation for high-speed electronic and optoelectronic applications. For instance, a GaAs-$Al_xGa_{1-x}As$ DBs operating at THz frequencies has been reported in Ref. [1].

Theoretical studies of the above systems usually neglect possible effects of disorder in order to simplify the analysis. However, carrier scattering by impurities or other point defects and rough interfaces decrease of electron mobility even in good-quality heterostructures [2]. Consequently,

*Corresponding author. Tel.: +34 91 394 44 88; fax: +34 91 394 45 47.
E-mail address: adame@fis.ucm.es (F. Domínguez-Adame).

0921-4526/$ - see front matter © 2005 Elsevier B.V. All rights reserved.
doi:10.1016/j.physb.2005.08.039

more elaborated approaches should take into account these imperfections to get a better understanding of tunneling process.

We developed a multichannel two-dimensional model to calculate vertical transport properties such as DC conductance and current in unintentionally disordered GaAs-$Al_xGa_{1-x}As$ DBs [3]. In this work, we extend the above model to include the effects of a magnetic field applied perpendicular to the system plane. The source of disorder comes from interface roughness at the heterojunctions. We model the interface roughness by protrusions of GaAs in $Al_xGa_{1-x}As$. The lateral and vertical sizes of the islands are stochastic variables with given average values ranging from few Angstroms up to few nanometers. Disorder break translational symmetry along the lateral direction and therefore electrons can be scattered off the growth direction. The model correctly describes channel mixing due to these elastic scattering events, yielding a reduction of the DC conductance in large systems. In this work we aim to elucidate the relationship between magnetotunneling properties of the DBS and microscopic parameters of the model (e.g. correlation length of the surface roughness). In particular, the applied magnetic field introduces a new length scale (the magnetic length) that competes with other spatial scales of the system, like the correlation length of the disorder. Thus, the interplay of different spatial scales could result in new phenomena that were not studied in previous works [3].

2. Discrete model

We restrict ourselves to a two-dimensional geometry for computational limitations, although the generalization to three dimensions is rather straightforward. We then consider the single-electron Schrödinger equation in the YZ plane within the framework of the one-band effective-mass approximation. Close to the Γ valley, this approach leads to the Ben Daniel–Duke equation for the envelope function $\chi(y,z)$

$$\left[-\frac{1}{2m^*}(\boldsymbol{p}+e\boldsymbol{A})^2+U(y,z)\right]\chi(y,z)=E\chi(y,z), \quad (1)$$

where $-e$ is the electron charge and z denotes the coordinate along the growth direction. We have taken a constant effective mass m^* at the Γ valley although this is not a serious limitation as the model can be easily generalized to include a position-dependent effective mass. $U(y,z)$ is the band-edge offset at position (y,z). The magnetic field $\boldsymbol{B}$ is applied along the X-direction, as shown in Fig. 1, and we can take the gauge $\boldsymbol{A}=(B/2)(0,-z,y)$.

We then consider a mesh with lattice spacings s_y and s_z in the Y- and Z-directions, respectively. Introducing the magnetic length $\ell_B \equiv \sqrt{\hbar/eB}$, the envelope function at mesh points $\chi(ms_y, ns_z) \equiv \chi_{m,n}$ is obtained after discretization of Eq. (1)

$$\begin{aligned}
&-\frac{\Delta_y^2}{s_y^2}\chi_{m+1,n}-\frac{\Delta_z^2}{s_z^2}\chi_{m,n+1}+\frac{1}{4\ell_B^4}(m^2s_y^2+n^2s_z^2)\chi_{m,n}\\
&+\frac{\mathrm{i}}{4\ell_B^2}\left[n\frac{s_z}{s_y}\Delta_y(\chi_{m+1,n}+\chi_{m,n})\right.\\
&\left.+m\frac{s_y}{s_z}\Delta_z(\chi_{m,n+1}+\chi_{m,n})\right]\\
&+\frac{2m^*}{\hbar^2}U_{m,n}\chi_{m,n}=\frac{2m^*}{\hbar^2}E\chi_{m,n}, \quad (2)
\end{aligned}$$

where the difference operators are $\Delta_y\chi_{m,n} \equiv \chi_{m,n}-\chi_{m-1,n}$ and $\Delta_z\chi_{m,n} \equiv \chi_{m,n}-\chi_{m,n-1}$.

After the discrete equation for the envelope function is obtained, the two-dimensional transfer-matrix approach can be used to calculate different physical quantities. The envelope functions within the contacts will be determined by the boundary conditions. These boundary conditions are open in the growth direction, and periodic in the lateral

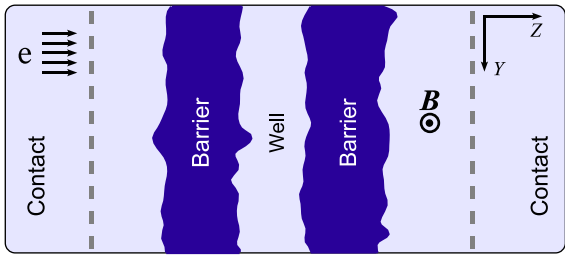

Fig. 1. Schematic view of the two barriers forming the heterostructure, showing the interface roughness. The magnetic field is applied along the X-direction, perpendicular to the system plane.

direction to minimize finite-size effects. The former implies plane wave solutions in the Z axis, and the latter yield an energy discretization on Y. As a consequence, this discretization results in a number of transverse channels equal to the number of segments in the transverse mesh direction. From the Landauer–Büttiker formalism [4], the zero temperature two-leads multichannel conductance can be calculated using de Fisher–Lee formula [5]. For brevity we omit the details that were already discussed in Ref. [3].

3. Interface roughness

Standard techniques, like scanning tunneling microscopy [6–8] and X-ray scattering [9], have been applied in recent years to quantitatively assess structural properties of multilayers. In particular, these techniques point out that unintentional disorder appearing during growth depends critically on the growth conditions and that the interfaces are not flat. As a consequence, translational symmetry in the plane perpendicular to the growth direction is broken. The numerical approach introduced above allows us to deal with realistic models of disorder in a rigorous way.

In order to treat electron scattering by interface roughness we have considered the formation of islands at the interface between two consecutive layers, having identical lateral sizes all of them and being consecutive one to each other. In our model, islands have heights that are randomly distributed (see Fig. 2).

Thus, it is possible to express the rough profile of the interface between two consecutive layers defining the following height function

$$h(y) = \eta \sum_n w_n\{\theta(y - n\zeta) + \theta[(n+1)\zeta - y] - 1\}. \tag{3}$$

Here $h(y)$ represents the deviation from the nominally flat surface at position y, θ is the Heavyside step-function, ζ is the island width, w_n is a random variable associated to the nth island that controls the fluctuation around the mean value, and η is the largest deviation—in absolute value—assuming that the w_n's are uniformly distributed between -1 and 1. Hereafter η will be referred to as magnitude of disorder.

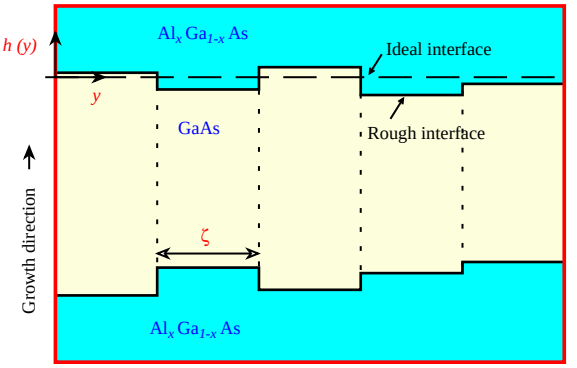

Fig. 2. Schematic view of a GaAs quantum-well with interface roughness, showing that the heterostructure can be regarded as an ensemble of ideal (flat interface) quantum-wells with random widths along the growth direction and size ζ along the lateral direction.

4. Numerical results

We have performed numerical calculations in order to study the effect of interface roughness on the transport properties of GaAs-$Al_xGa_{1-x}As$ DBS. In what follows the conductance G will be expressed in units of $G_0 \equiv 2e^2/h$. The effective mass is taken to be $m^* = 0.067m$, m being the free electron mass. The barrier height is set 0.30 eV, corresponding to 35% Al mole fraction. The lattice spacings are $s_y = 10.0$ nm and $s_z = 0.3$ nm.

4.1. Flat interfaces

Before considering the effects of disorder, it is illustrative to study the magnetotunneling effect in the case of ideal (flat) interfaces of the DB. In the absence of disorder and magnetic field, the conductance at zero temperature displays a single resonance peak below the barrier due to the occurrence of a single quasi-bound state at the quantum-well. The peak shifts upwards and broadens as the magnetic field increases and finally it splits into a series of equally-spaced resonances when the field exceeds a critical value. Fig. 3 shows

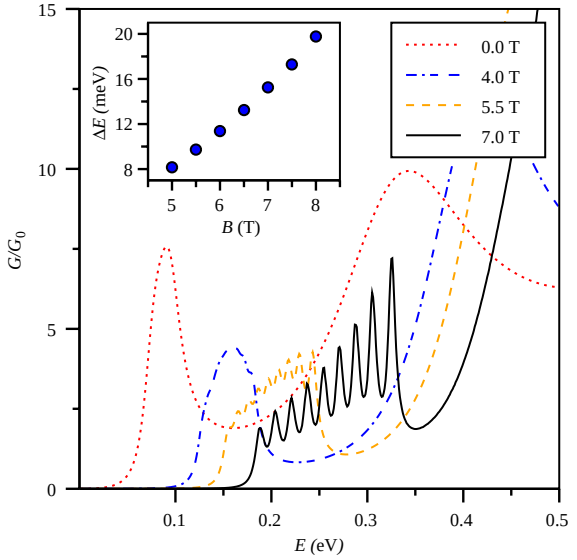

Fig. 3. Normalized conductance as a function of the Fermi energy for different values of the magnetic field. The interfaces of the DB are flat. The widths of the barriers and the quantum-well are 2.1 and 4.8 nm, respectively. The inset shows the dependence of the level spacing on the magnetic field.

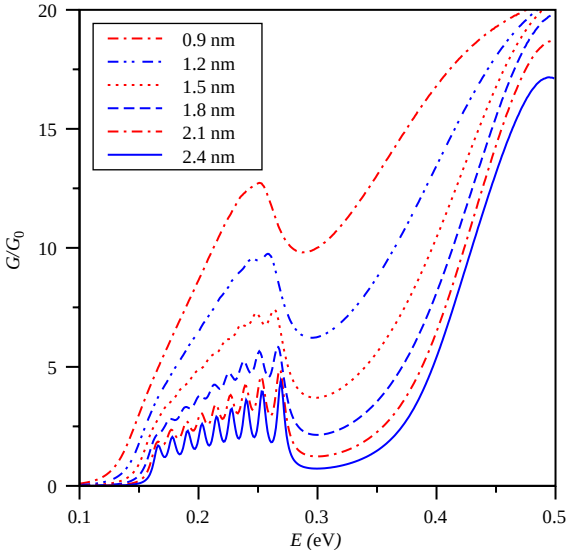

Fig. 4. Normalized conductance as a function of the Fermi energy for different values of the barrier widths, indicated in the legend. The interfaces of the DB are flat. The magnetic field is $B = 6.0$ T and a quantum-well width of 4.8 nm.

the results when the widths of the barriers and the quantum-well are 2.1 and 4.8 nm, respectively.

The conductance peaks at high field are equally spaced, and their number equals the number of channels. The energy spacing is found to increase almost linearly with the magnetic field, as shown in the inset of Fig. 3. The energy spacing is 17 meV for $B = 7.0$ T in the DB with the chosen parameters. However, this energy spacing also depends on the lattice spacing, namely the larger the lattice spacing, the larger the energy spacing. Thus, we will refer to *lattice Landau levels* (LLL) hereafter.

Conductance curves depend also on the geometry of the sample. Fig. 4 shows the conductance as a function of the Fermi energy for $B = 6.0$ T and a quantum-well width of 4.8 nm. Different curves correspond to various barrier widths, indicated in the legend. The LLL can be resolved when the barriers are wide enough, while for narrow barriers the levels merge into a structureless and broad peak. This behaviour can be understood from basic tunneling effects. The narrower the barriers, the larger the coupling of the quasi-bound state to the continuum, thus increasing its energy width.

Similar effects should appear by varying the quantum-well widths since the narrower the quantum-well, the higher the energy of the quasi-bound state, thus increasing the coupling to the continuum. Fig. 5 shows the expected results for DBs whose barrier widths are 2.1 nm and the magnetic field is $B = 6.0$ T. It is apparent that LLL are resolved only for wide quantum-wells, where the coupling of the quasi-bound state to the continuum is smaller, thus decreasing its energy width. Also notice that the average value of the conductance for Fermi energy below the energy barrier (0.3 eV) increases when decreasing the quantum-well width. This effect is due to the increase of the transmission coefficient when increasing the coupling to the continuum. A similar effect is already observed by reducing the barrier width (see Fig. 4).

4.2. Rough interfaces

Once we have discussed LLL in DBs with flat interfaces, we now consider the effects of interface

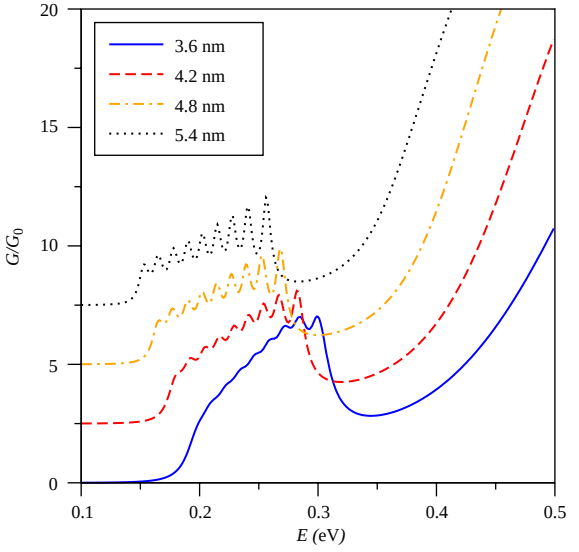

Fig. 5. Normalized conductance as a function of the Fermi energy for different values of the quantum-well widths, indicated in the legend. The interfaces of the DB are flat. The magnetic field is $B = 6.0\,\mathrm{T}$ and a barrier width of 2.1 nm. Curves are shifted upwards to improve the clarity of the plot.

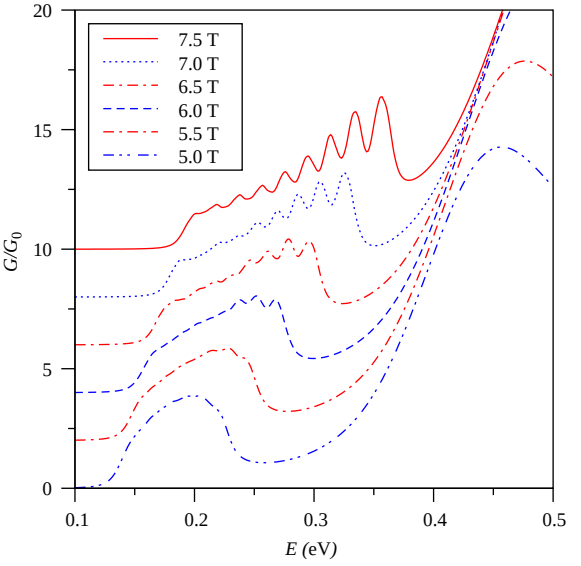

Fig. 6. Normalized conductance as a function of the Fermi energy for different values of the magnetic field. The nominal widths of the barriers and the quantum-well are 2.1 and 4.8 nm, respectively. The lateral and size of the islands is $\zeta = 10\,\mathrm{nm}$ and the magnitude of disorder is $\eta = 0.3\,\mathrm{nm}$. Curves are shifted upwards to improve the clarity of the plot.

roughness, characterized by the magnitude of disorder η and lateral size of the islands ζ given in Eq. (3). Hereafter the conductance curves comprise the average of 400 realizations of the disorder.

According to the model of disorder introduced above, the DB with interface roughness can be regarded as an ensemble of ideal (flat interface) quantum-wells and barriers with random widths and size ζ along the lateral direction. This is schematically shown in Fig. 2. The fluctuation in the epilayer (GaAs and $Al_xGa_{1-x}As$) widths results in a random distribution of the couplings of the local quasi-bound states and the continuum. This randomness finally results in the broadening of the resonant level (inhomogeneous broadening). Therefore, larger fields should be applied to observe LLL, as compared to ideal DBs with flat interfaces. Fig. 6 displays the normalized conductance when the nominal widths of the barriers and the quantum-well are 2.1 nm and 4.8 nm, respectively. The lateral size of the islands is $\zeta = 10\,\mathrm{nm}$ and the magnitude of disorder is $\eta = 0.3\,\mathrm{nm}$ (one monolayer). LLL are observed when the magnetic field is larger than 6.5 T, whereas they are resolved when $B = 5.5\,\mathrm{T}$ in ideal DBs (see Fig. 3). This result confirms our qualitative reasoning introduced above.

Fig. 7 demonstrates that disorder smears out the LLL as expected. For a fixed magnetic field, the increase of the magnitude of disorder (Fig. 7a) or the lateral size of the islands ζ (Fig. 7b) results in a single structureless conductance peak.

5. Conclusions

In this paper we have numerically studied magnetotunneling transport in a multichannel two-dimensional DBs. To this end, we have extended a previous method [3], based on a discrete Ben Daniel–Duke equation, to include an applied magnetic field. In particular we have focused on the effects of unintentional disorder (interface roughness) on magnetotunneling transport. When disorder is negligible, the conductance presents a single resonance peak below the barrier.

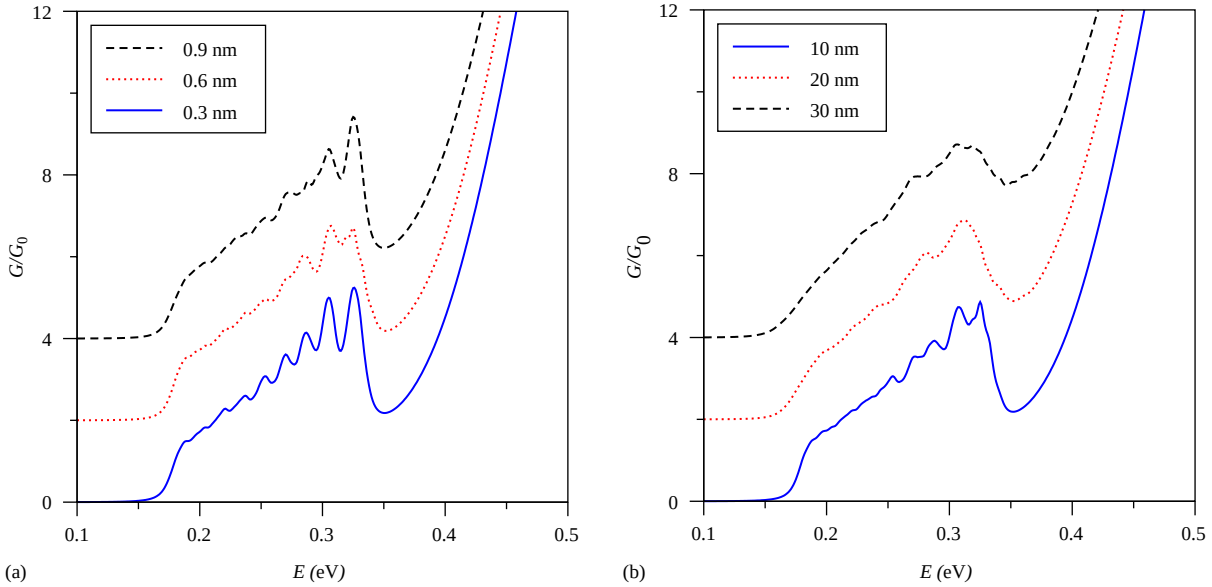

Fig. 7. Normalized conductance as a function of the Fermi energy for $B = 7.0$ T. The nominal widths of the barriers and the quantum-well are 2.1 and 4.8 nm, respectively. (a) $\zeta = 10$ nm and different values of η. (b) $\eta = 0.6$ nm and different values of ζ. Curves are shifted upwards to improve the clarity of the plot.

The peak shifts upwards and broadens as the magnetic field increases and finally it splits into a series of equally-spaced resonances when the field exceeds a critical value. The level spacing is proportional to the magnetic field, then being related to Landau splitting. Disorder tends to mask the splitting, although well resolved peaks appear for moderately high field and realistic values of the disorder. The present model provides a qualitative picture of the effects of lateral disorder on the conductance. Therefore, our results are the starting point for further developments, including electron–electron and electron–phonon coupling.

Acknowledgements

The authors thank I. Gómez for helpful comments. Work at Madrid was supported by DGI-MCyT (Project MAT2003-01533) and CAM (Project GR/MAT/0039/2004). E. Diez was supported by the program "Ramón y Cajal", MEC (Project FIS2005-01375) and JCyL (Project SA007B05).

References

[1] T.C.L.G. Sollner, W.D. Goodhue, P.E. Tannenwald, C.D. Parker, D.D. Peck, Appl. Phys. Lett. 43 (1984) 588.
[2] U. Penner, H. Rücker, I.N. Yassievich, Semicond. Sci. Technol. 13 (1998) 709.
[3] I. Gómez, E. Diez, F. Domínguez-Adame, P. Orellana, Physica E 18 (2003) 372.
[4] R. Landauer, IBM J. Res. Dev. 1 (1957) 223;
M. Büttiker, Phys. Rev. Lett. 57 (1986) 1761;
M. Büttiker, IBM J. Res. Dev. 32 (1988) 63;
M. Büttiker, IBM J. Res. Dev. 32 (1988) 317.
[5] D. Fisher, P.A. Lee, Phys. Rev. B 23 (1981) 6851.
[6] R.M. Feenstra, D.A. Collins, D.Z.-Y. Ting, M.W. Wang, T.C. McGill, Phys. Rev. Lett. 72 (1994) 2749.
[7] H.W. Salemik, O. Albrektsen, P. Koenraad, Phys. Rev. B 45 (1992) 6946.
[8] S. Gwo, K.-J. Chao, C.K. Shih, K. Sandra, B.G. Streetman, Phys. Rev. Lett. 71 (1993) 1883.
[9] M. Jergel, V. Holý, E. Majková, Š. Luby, R. Senderák, H.J. Stock, D. Menke, U. Kleineberg, U. Heinzmann, Physica B 253 (1998) 28.